Electrical conductivity and seismic velocity of the martian mantle: Signatures of large meteorite impacts

Thomas Ruedas[1,2*], Doris Breuer[2]

[1]*Impact and Meteorite Research, Museum für Naturkunde Berlin*

[2]*Institute of Planetary Research, German Aerospace Center (DLR), Berlin*

[*]Corresponding author email: thomas.ruedas@mfn.berlin

Model setup

We model the thermochemical evolution of a Mars-like planet with a modified version of the mantle convection code StagYY (Tackley, 2008) coupled to a petrological and mineral physics model of the mantle and core materials to determine its physical properties and melting behavior (cf. Ruedas and Breuer, 2017). Starting at 4.4 Ga, the models evolve undergoing compositional changes due to melting; furthermore, a large, basin-forming impact of the magnitude of the Utopia-, Isidis-, or Huygens-forming event is included at 4 Ga and causes further local melting and heating of the mantle, producing major thermal and compositional anomalies. The impact is implemented in a simplified, parameterized form that focuses on describing the first-order effects caused by shock-heating in the surroundings of the impact site (e.g., Watters *et al.*, 2009). The final result of a typical modeling run is a model of the present-day thermal and compositional state of the martian interior, in particular of the mantle.

Model properties

Mantle: Initial potential temperature: 1700 K; initial T step across CMB: 150 K; 15fold viscosity increase between upper and lower half of mantle; radionuclide concentrations from Wänke and Dreibus (1994), Mg#=0.75, 36, 72, or 144 wppm water; melting included, threshold for melt extraction: 0.7%; liquid iron–sulfur (16 wt.% S) alloy core (R_c = 1730 km), no basal bridgmanite+ferropericlase layer in the mantle; duration: 4.4 Gy

Impacts: S-type asteroid impactor, 2720 kg/m^3, 9.6 km/s, striking at 4 Ga at an angle of 45°; Utopia-sized (final crater diameter: 3380 km, impactor diameter: 699 km), Isidis-sized (final crater diameter: 1352 km, impactor diameter: 244 km), or Huygens-sized (final crater diameter: 467 km, impactor diameter: 70.6 km)

Model evolution and dynamics

With time the planetary interior cools in all models, and convective vigor as expressed by the root-mean-square velocity decreases; the vigor is higher in models with a higher water content. A depleted, less dense layer forms at the base of the lithosphere and reduces convective motion in the melting region.

Impacts provide an instantaneous input of energy that temporarily disturbs this otherwise stable layering, the more the larger the impact. In our models we assume that almost all of the melt generated by the impact is extracted instantaneously and forms new crust at the surface, leaving back a strongly depleted mantle residue (Fig. 1). In the impact basin, the melt is assumed to fill preexisting pore space, which has a significant effect on various physical properties. The strong thermal and compositional impact-generated mantle anomalies spread out at the base of the lithosphere, where they may be stabilized and preserved as a long-term feature of the uppermost mantle (Fig. 2), mostly due to their long-lived compositional buoyancy. Preservation is achieved well only in the models with low water content, whereas the greater vigor in the more water-rich models leads to a stronger erosion of the anomaly. At low water contents, this effect may provide a mechanism that produces long-lived chemical heterogeneities in the martian mantle.

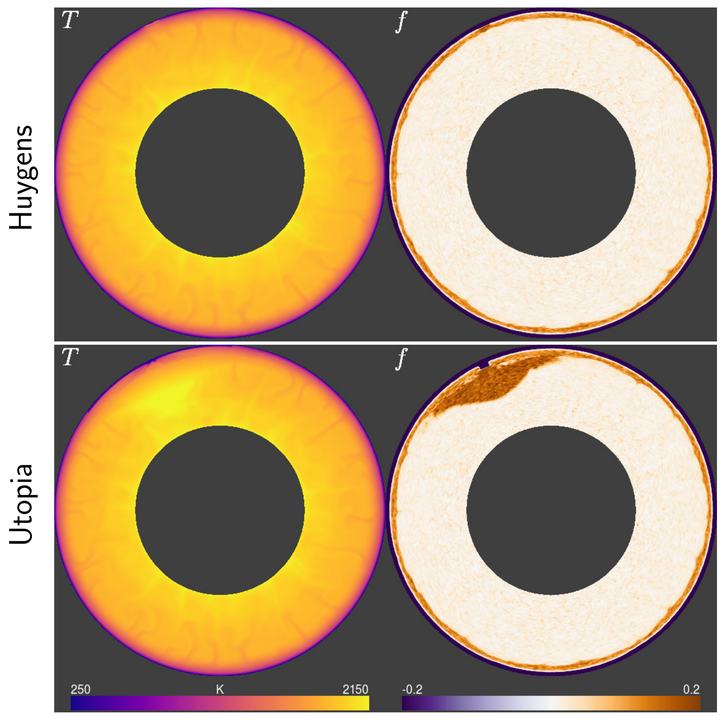

← **Fig. 1:** Temperature T and composition/depletion f at the time of impact, for the Huygens-sized and the Utopia-sized events from the models with 36 ppm initial bulk mantle water. The impact site is near the 11 o'clock position of the cross-section.

↓ **Fig. 2:** Snapshots of the models with 36 wt.ppm initial water and with a Huygens-size (upper row) or a Utopia-size (lower row) impact. Each row shows the present-day distributions of T and f as well as the density anomaly ($\Delta\varrho$), the bulk sound speed anomaly (Δv_B), and the anomaly of the decadic logarithm of the electrical conductivity ($\Delta(\lg\sigma)$). The color scales are clipped to improve the visibility of structures.

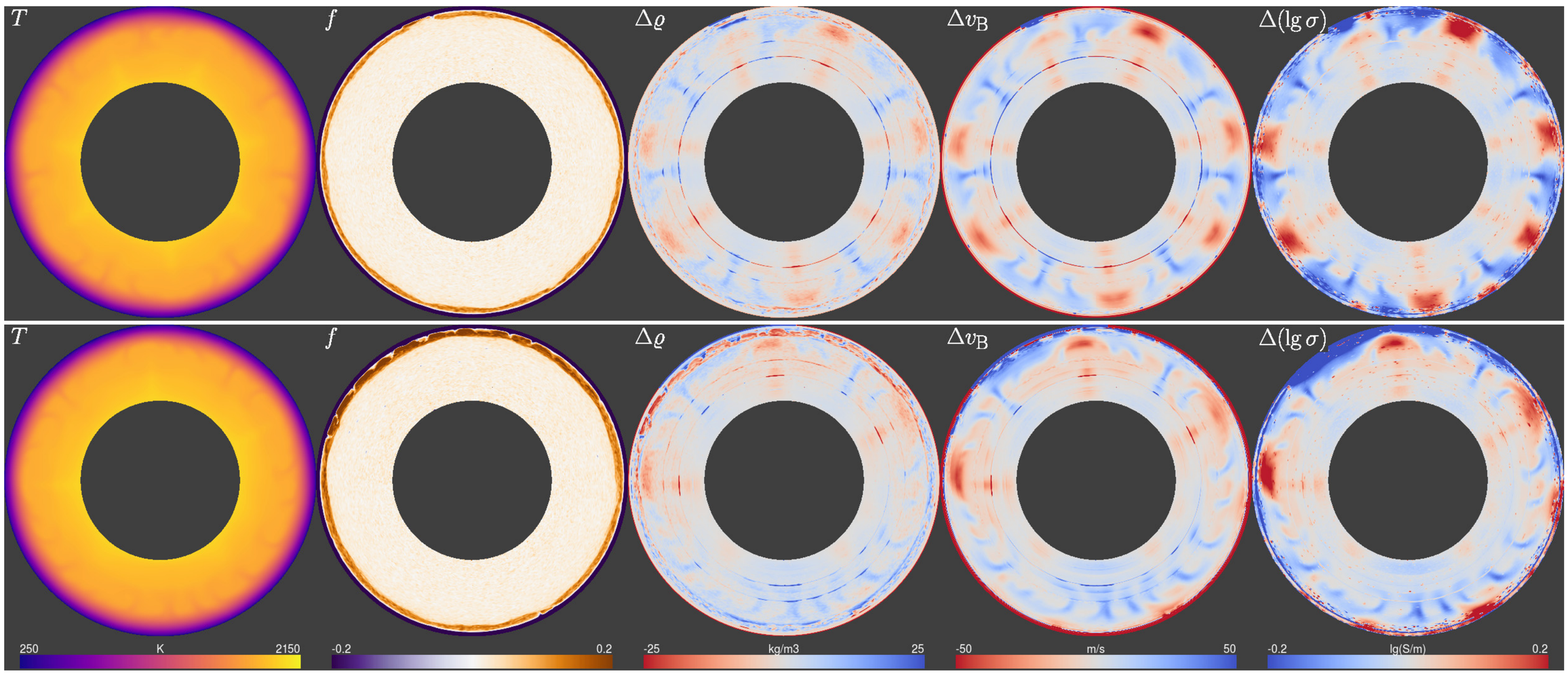

Results: Observables

The integration of a mineralogical and geochemical model into convection calculations permits the self-consistent prediction of many geophysical observables. Fig. 3 shows depth profiles of the temperature T, depletion f, density ϱ, bulk sound speed $v_B = \sqrt{K_S/\varrho}$, and electrical conductivity σ.

The increased depletion in iron and water caused by impacts modifies the density and electrical conductivity of the target and thus produces low-density and low-conductivity anomalies that are expected to be visible in gravity measurements and electromagnetic soundings; detection by seismic means, however, would be possible only under very favorable conditions with a local network. Expected gravity anomalies are on the order of a few hundred mgal and hence compatible with those observed at Isidis and Utopia, but not at Huygens (Genova *et al.*, 2016). The full pattern of density, velocity, and conductivity anomalies (Fig. 2) results from the thermal and compositional heterogeneities in the mantle. Note that the crustal thickness determined from satellite altimetry can be locally underestimated by several kilometers if impact-induced lateral density anomalies in the crust or mantle are neglected.

The bulk velocity shown here can be derived from seismic observations via $v_B = \sqrt{v_P^2 - \frac{4}{3}v_S^2}$, but the P-wave and S-wave velocities from InSight could also be derived directly from the mineral physics model. The electrical conductivity can be inferred from magnetometer data. MGS data (Civet and Tarits, 2014) yield a higher mantle conductivity than our models, pointing to higher water contents and/or temperatures than assumed here; the crust in particular may hold substantial amounts of water in pores. Of the observables, the conductivity is the most sensitive to water content and may thus help constrain the water content of the martian mantle.

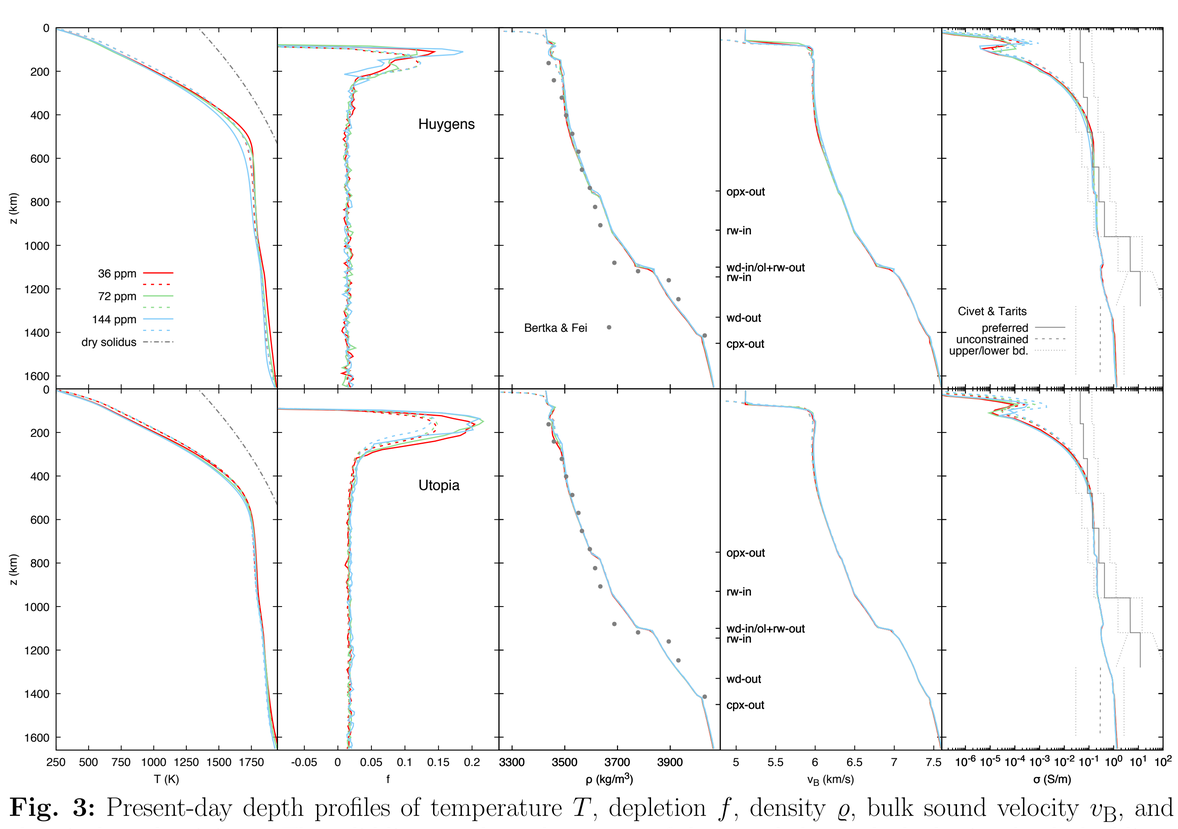

Fig. 3: Present-day depth profiles of temperature T, depletion f, density ϱ, bulk sound velocity v_B, and electrical conductivity σ. The solid lines are lateral averages of the mantle beneath the basin, the dashed lines are global averages. Also shown are the solidus of dry martian peridotite and independent experimental or observational constraints on $\varrho(z)$ (Bertka and Fei, 1998) and $\sigma(z)$ (Civet and Tarits, 2014).

References

Bertka, C. M., Y. Fei (1998). *Earth Planet. Sci. Lett.*, *157*, 79–88.

Civet, F., P. Tarits (2014). *Earth Planets Space*, *66*, 85.

Genova, A., S. Goossens, F. G. Lemoine, *et al.* (2016). *Icarus*, *272*, 228–245.

Ruedas, T., D. Breuer (2017). *J. Geophys. Res.*, *122*, 1554–1579.

Tackley, P. J. (2008). *Phys. Earth Planet. Inter.*, *171*, 7–18.

Wänke, H., G. Dreibus (1994). *Phil. Trans. R. Soc. Lond.*, *A 349*, 285–293.

Watters, W. A., M. T. Zuber, B. H. Hager (2009). *J. Geophys. Res.*, *114*, E02001.